

Article

Effect of Tool Rotation Direction on Mechanical Strength of Single Lap Friction Stir Welded Joints between AA5083 Aluminum Alloy and S355J0 Steel for Maritime Applications

Guido Di Bella , Chiara Borsellino, Amani Khaskhoussi  and Edoardo Proverbio 

Department of Engineering, University of Messina, Contrada di Dio 1, 98166 Messina, Italy

* Correspondence: guido.dibella@unime.it; Tel.: +39-090-676-5310

Abstract: This study aims to investigate a friction stir welded joint between steel and aluminum alloy that is employed in maritime applications (i.e., connection between the ship over-structures and the hull or deck). By changing the tool rotational direction, or the advancing or retreating side, a single lap configuration was studied. Tensile tests were conducted to evaluate the mechanical resistance and the surface fracture after a preliminary investigation consisting of morphological and microstructural analyses and microhardness measurements, with the goal of considering the possibility of replacing the typical joining processes, such as traditional welding or explosion welding, with friction stir welding. The testing showed that the joint produced on the advancing side performed better (+23.5% of the maximum load) than the joint made on the retreating side.

Keywords: joining; FSW; shipbuilding; aluminum; steel



Citation: Di Bella, G.; Borsellino, C.; Khaskhoussi, A.; Proverbio, E. Effect of Tool Rotation Direction on Mechanical Strength of Single Lap Friction Stir Welded Joints between AA5083 Aluminum Alloy and S355J0 Steel for Maritime Applications. *Metals* **2023**, *13*, 411. <https://doi.org/10.3390/met13020411>

Academic Editor: António Bastos Pereira

Received: 12 January 2023

Revised: 9 February 2023

Accepted: 12 February 2023

Published: 16 February 2023



Copyright: © 2023 by the authors. Licensee MDPI, Basel, Switzerland. This article is an open access article distributed under the terms and conditions of the Creative Commons Attribution (CC BY) license (<https://creativecommons.org/licenses/by/4.0/>).

1. Introduction

Aluminum alloys have grown in popularity over the last decade due to their unique properties that make them more competitive than other metallic materials such as steel. Particularly, their lightness, good mechanical properties, high ductility, and corrosion resistance make them suitable for many applications in the transport field (i.e., automotive, aerospace, and naval) [1–3].

In marine applications, aluminum alloys can be used, for example, to make a whole ship: some years ago, the transportation enterprise Liberty Lines built in its own shipyard in Trapani (Sicily), the world's largest hydrofoil using the aluminum alloy AA6082-T6. Figure 1 illustrates two stages of construction by showing the hull, which is made of fully welded aluminum sheets. The high level of surface finishing that results from a particular method of making the weld beads may be seen. Particularly, in a hydrofoil, the weight is entirely supported by the submerged part of the wings. For this, the main structures (i.e., hulls and wings) must respect more severe weight thresholds than those of other speed vessels. Consequently, it is needed, first, to focus attention on the compromise between the low thicknesses of the hull sheets and the good mechanical properties, and second, to design the shape of the wings to guarantee efficiency and seakeeping. Aluminum alloys allow for containing the weights and optimizing the design [4,5].

Also, in the military field, aluminum alloys are used to make faster and more efficient ships. In 2020–2021, Intermarine built in its shipyard in Messina (Sicily) two patrol boats, designed to be self-straightening and unsinkable. These are the longest ships of this type ever built in Italy, with an aluminum alloy hull of 33.60 m in length and 8.15 m in width with a fully loaded displacement of about 150 t.

Aluminum alloys can be coupled to other metallic materials, such as steel. Generally, steel is used to make the hull and aluminum to make the over-structures. This allows for both weight reduction and increased stability by lowering the ship's center of gravity. Examples of this coupling between aluminum and steel include the 1999-built passenger/ro-ro

cargo ships “Isola di Stromboli” and “Isola di Vulcano,” which are used by the transportation company Caronte & Tourist to connect Sicily to the smaller islands (such as Lipari). Additionally, Fincantieri uses the advantages of aluminum alloy to replace steel in the over-structures of cruise ships.

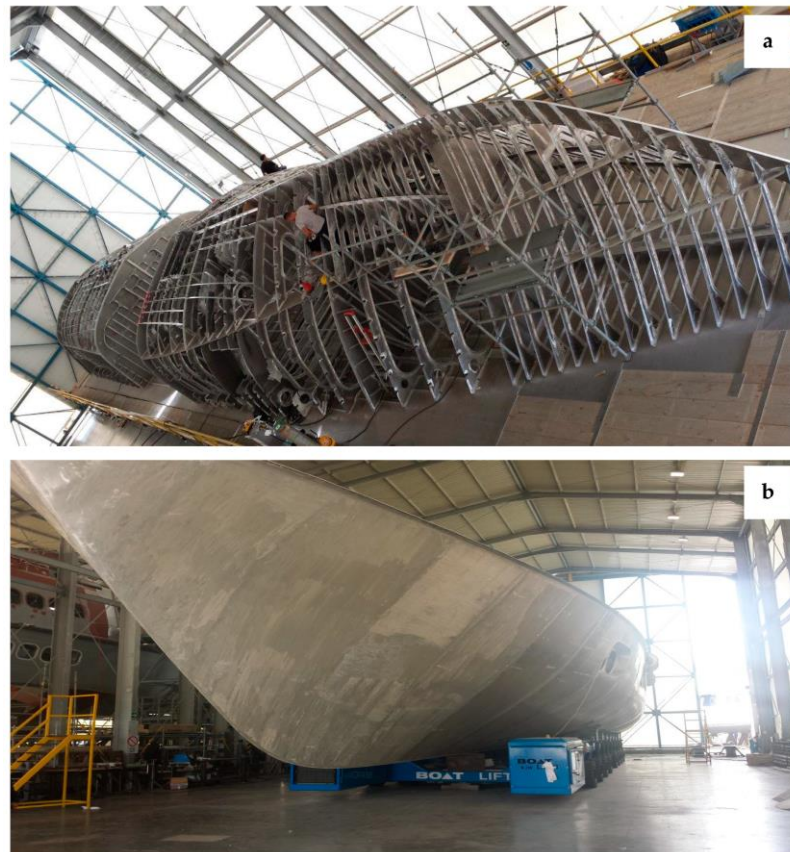


Figure 1. The hull of the largest hydrofoil in the world is being built in two stages: (a) building the frame and (b) covering the frame with aluminum planking.

With the rapid development of the advanced manufacturing industry, interest in these multi-material hybrid components is growing due to several advantages, including weight reduction and economics [6].

Typically, fusion welding methods are used for joining steel sheets. Unfortunately, these techniques show significant drawbacks when they are applied to join aluminum and steel. In fact, during the joining process, it is possible to observe the formation of inter-metallic compounds that are characterized by a low plastic deformability, generating a brittle joint. Moreover, the molten aluminum shows low wettability on the solid steel.

This necessitates the investigation of new fusion welding techniques or the use of other joining techniques to connect aluminum and steel.

Among the technologies of fusion welding, the most promising are plain resistance spot welding, resistance spot welding with a cover plate, resistance spot welding with an interlayer, resistance element welding, laser beam welding, and arc welding.

However, solid-state welding represents the more suitable method to join these two metals. This includes the following technologies that provide a direct metal-to-metal contact with adequate pressure to generate a performant joint without the production of inter-metallic compounds: explosion welding and transition joints, magnetic pulse welding, roll bonding, friction stir welding (FSW), friction bit joining, and ultrasonic spot welding [7].

Among these technologies, friction stir welding is energy-efficient, environment-friendly, and versatile [8]. Due to these characteristics, it has developed very rapidly in

recent years in many industrial fields. Particularly, the automotive industry has been the first sector where it has been introduced to join steel and aluminum [9–11].

The process is simple, and different joint configurations can be possible, i.e., lap and butt. A machine-driven die pushes a non-consumable rotating tool into the workpiece. This consists of a pin that penetrates the material and a shoulder that is in contact with the metal surface. The tool has two functions: (i) heating and (ii) mixing. Heating is generated both by the friction between the tool and the workpiece and by the plastic deformation of the workpiece. It softens the materials around the pin, promoting mixing during the movement of the tool, which rotates and translates. As a result, the joint is created [12].

Many shipbuilding companies, including Fincantieri, have recently concentrated their efforts on this technology to join the aluminum components for over-structures with the steel hull by establishing specialized tasks in research programs supported by national and regional public organizations (i.e., the Italian Ministry or the Sicilian Region).

In this work, a single lap friction stir welded joint between the aluminum alloy (AA5083-H111) and the steel sheet (S355-J0) by investigating the effect of the direction of rotation of the tool: (i) AS, when the advancing side is by the side of the steel (lower plate), and (ii) RS, when the retreating side is by the steel side (lower plate) (see Figure 2) [13,14]. As a preliminary step, a microstructural study was performed, and then tensile tests were carried out to evaluate the joint strength.

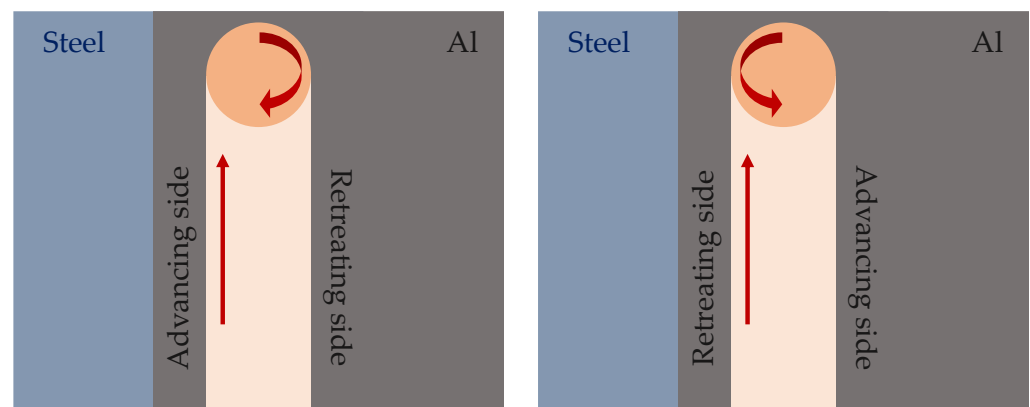


Figure 2. Advancing and Retreating sides.

2. Experimental Setup

2.1. Materials

The friction stir welded joints were made by coupling AA5083-H111 aluminum alloy sheets of 6 mm thickness, supplied by Media Metalli (www.mediametalli.com, Italy), and S355-J0 steel sheets of 5 mm thickness, supplied by Fincantieri shipyard of Palermo (www.fincantieri.com, Italy). To meet the needs of the Fincantieri shipyard, which joins this aluminum and steel to lighten the over-structures in the construction of the cruise ships, materials and thicknesses were identified.

AA5083 is a non-heat treatable alloy that is used in a variety of applications, including shipbuilding, railway, and automotive. It is only strengthened by strain hardening due to the cold forming. The H111 condition was obtained during subsequent operations such as stretching or levelling. The result is an annealed and slightly strain-hardened (less than H11 temper) alloy. S355-J0 is an unalloyed carbon structural steel suitable for cold forming. It is used in many different fields, such as naval carpentry, the production of metal structures, the construction of tanks, architecture, etc. J0 means that, at a temperature of 0 °C, the minimum impact energy is equal to 27 J.

Preliminary tests (i.e., tensile tests and microhardness measurements) were performed to evaluate the main properties of aluminum and steel. Particularly, Tables 1 and 2 summarize, respectively, the chemical composition and the main mechanical properties for both materials.

Table 1. Chemical composition of AA5083-H111 aluminum alloy and S355-J0 steel (wt. %).

	Al	Mg	Mn	Si	Fe	Cr	Zn	C	T	Cu	S	P	N	Other
AA5083-H111	Bal.	4.0–4.9	0.4–1.0	<0.4	<0.4	0.05–0.25	<0.25	-	<0.15	<0.1	-	-	-	<0.15
S355-J0	-	-	<1.60	<0.55	-	-	-	<0.20	-	<0.55	<0.03	<0.03	<0.012	-

Table 2. Mechanical properties of AA5083-H111 aluminum alloy [15] and S355-J0 steel.

	R _m [MPa]	R _{p02} [MPa]	A [%]	HV _{0.5}
AA5083-H111	300	170	27	52
S355-J0	505	350	22	150

2.2. Joining Process

The friction stir welded joints were manufactured by RIFTEC (RIFTEC GmbH, Geesthacht, Germany) [16] with a three-axis CNC Fritz Werner milling machine (FRITZ WERNER Industrie-Ausrüstungen GmbH, Geisenheim, Germany). Firstly, aluminum and steel plates having 150 × 500 mm sizes were overlapped for the whole length and for a width of about 50 mm to obtain a single lap configuration. Then, a special tool was rotated and moved on the aluminum sheet across the length of overlapping both in retreating and in advancing side to promote the connection.

Particularly, the tool is constituted by a shoulder having a diameter of 25 mm and a three flat sided pin having 18 mm size at root, 12 mm size at tip, and 6 mm height to promote the tool sinking into the whole thickness of the aluminum sheet until it reaches the steel. The inclination of the tool is equal to 0°. It is made of high carbon steel, characterized by high yield strength to prevent plastic deformation during the process, excellent abrasion resistance, and high resistance to heat oxidation. Figure 3 reports a focus on the Friction Stir Welded area. Particularly, it shows:

- the whole structure constituted by the two plates of steel (left or bottom in all Figures) and aluminum alloy;
- a zoom on the aluminum area involved by the tool stirring;
- a section after cutting;
- the section after mechanical and etching treatment. In this last, steel inclusions in the aluminum alloy are evident and the lines with the micro-hardness measurements are drawn;
- an optical microscope image that highlights the steel inclusions.

Moreover, a section of the joint evidencing the aluminum (upper sheet) and the part of steel subjected to welding process (aluminum/sheet interface) can be observed in [16].

The process was carried out at a welding speed of 300 mm/min at 400 rpm and with a force control of 30 kN, by changing the rotation direction of the tool (i.e., advancing and retreating).

2.3. Testing

2.3.1. Single-Lap Shear Test

The joints were mechanically characterized through a ZwickRoell Z600 testing machine (ZwickRoell Srl, Genoa, Italy), equipped with a 10 kN load cell, in accordance with UNI EN ISO 12996. The crosshead rate was set to 1 mm/min. For each configuration (i.e., advancing and retreating), five samples were tested.

2.3.2. Hardness Test

Microhardness was measured on cross-sections extracted from the middle of the welds. The Vickers hardness measurements were carried out using the FUTURE-TECH FM-300e with a load of 500 g. In accordance with the ASTM E384-17 standard, a minimum

spacing distance between two indentations of 2.5 times the value of the indent diagonal was respected. For each cross section (i.e., AS and RS), three profiles were carried out.

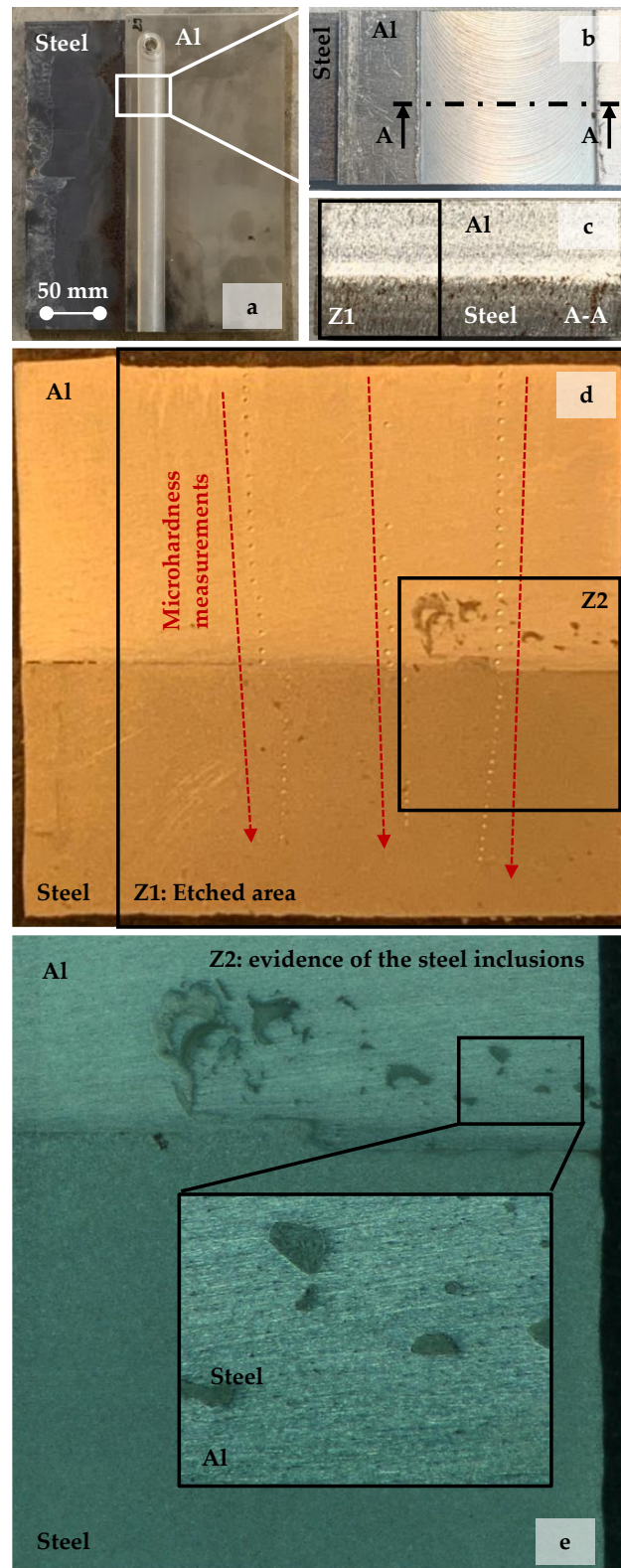


Figure 3. Focus on Friction Stir Welded area: (a) whole joined structure; (b) zoom on the aluminum area involved by the tool; (c) section after cutting; (d) treated area (mechanical and etching); (e) optical microscope image of the steel inclusions.

2.3.3. Metallography

The FUTURE-TECH FM-300e optical microscope (Future-Tech Corp, Kawasaki, Japan) and a SEM-FIB Zeiss Cross Beam 540 microscopy (Zeiss, Oberkochen, Germany) were used for morphological and microstructural analysis.

3. Results and Discussion

3.1. Single-Lap Shear Test

Figure 4 reports the load-displacement curves for all the investigated samples, i.e., AS and RS. These are characterized by the same trend, and they are almost overlapping. For all the samples, the curve is characterized by two regions with different slopes.

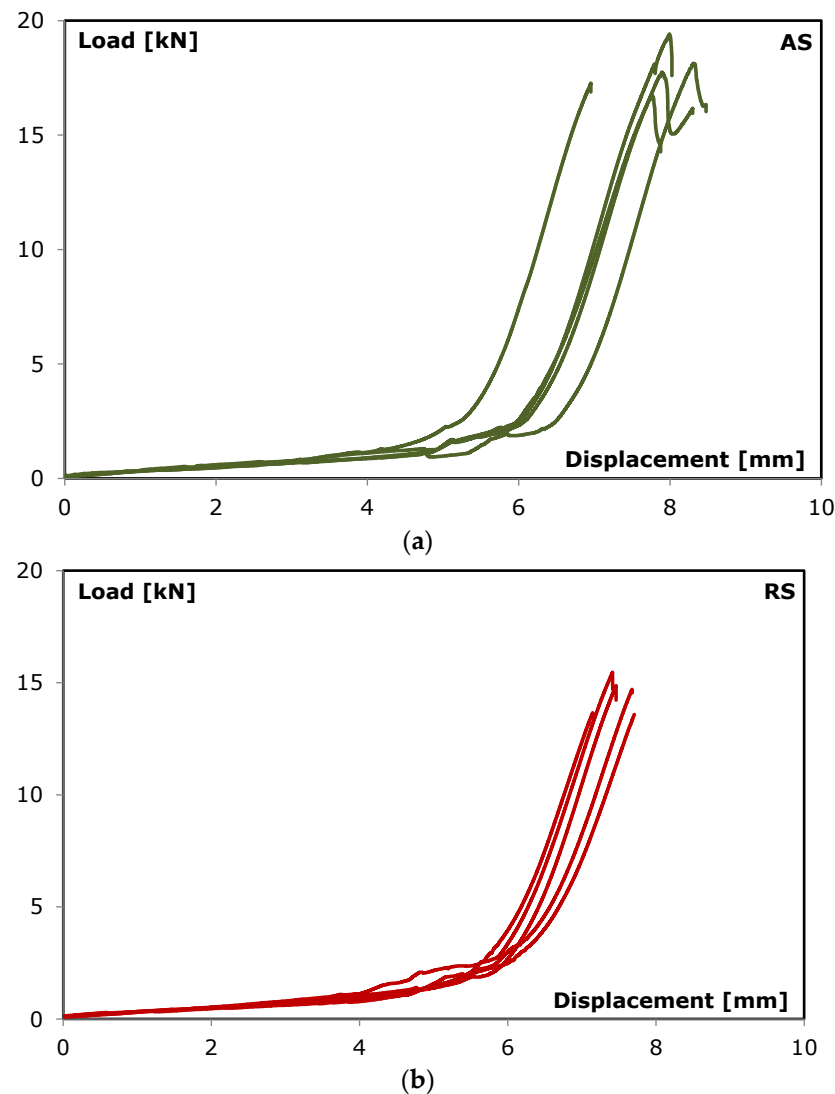


Figure 4. Load-displacement curves, respectively, for (a) advancing and (b) retreating side joint.

Firstly, the load slightly increases due to small settlements in the areas around the weld. Then, for a displacement of about 6 mm, almost the same for all the samples, the load abruptly increases until it reaches the maximum value corresponding to the failure of the joint.

The typical failure mode of both single lap friction stir welded joint is shown in Figure 5. Particularly, it is possible to observe the joining area between the steel and the aluminum generated by the action of the pin that rotates and moves along the contact zone by promoting the welding. The lines produced by the movement of the tool are well evident. The width of this area is equal to 10 mm.

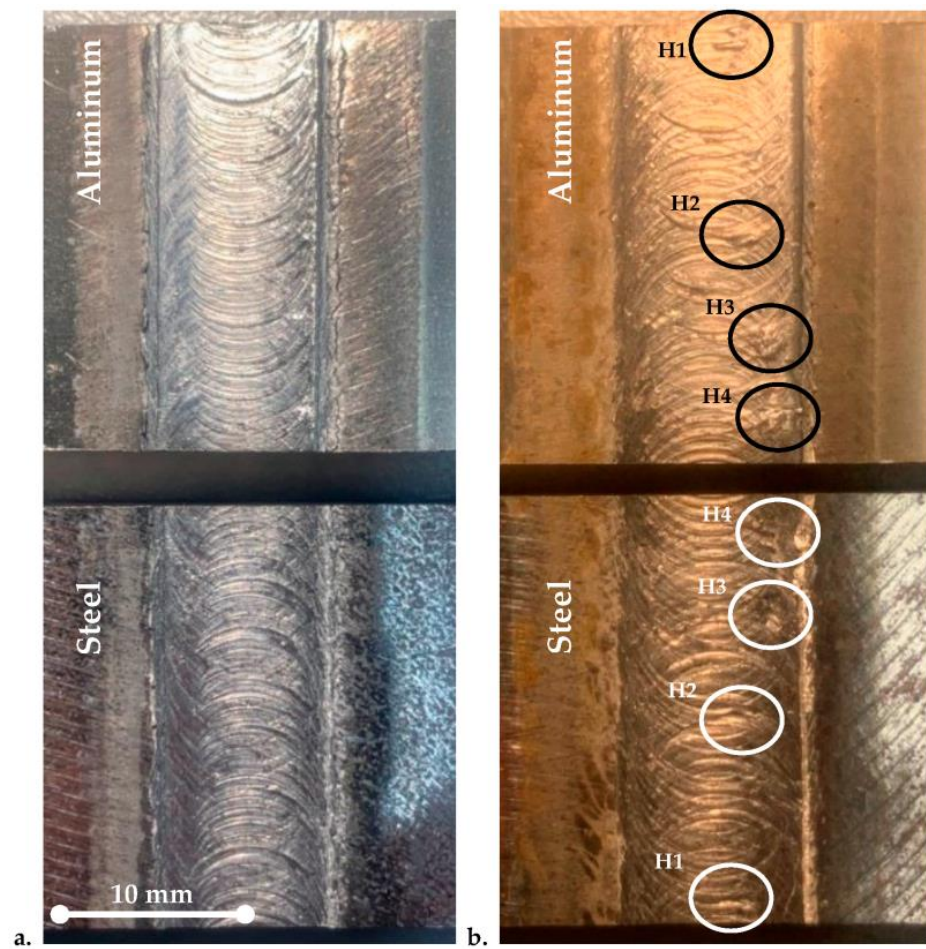


Figure 5. Failure surface of: (a) AS joint; (b) RS joint (the circles indicate the local hooks).

The ratio between the load “P” and the area “A” defined by this last width and the sample length [17] can be identified as a shear stress. Especially, Figure 6 shows the boundary conditions during the tensile test on the connection plane between the two sheets by also evidencing the fracture area that corresponds to the zone where the material mixing occurs.

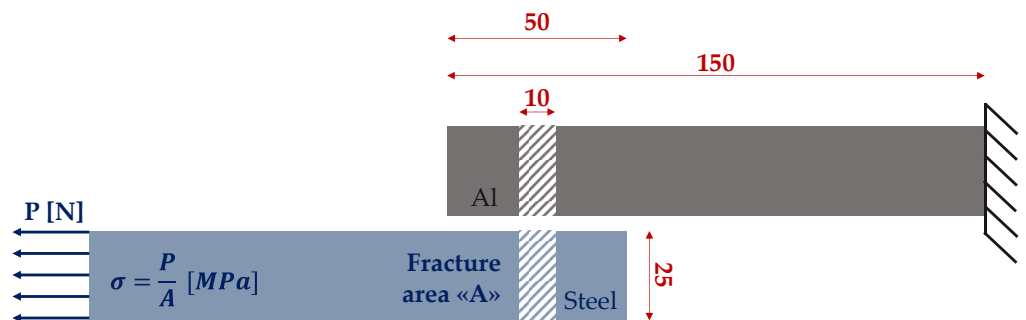


Figure 6. Boundary condition on the Al/Steel connection plane (U.M. = [mm]).

Figure 7 depicts a comparison of the shear stresses of the two types of joints (AS and RS). It is possible to observe that the samples AS are characterized by a higher stress value.

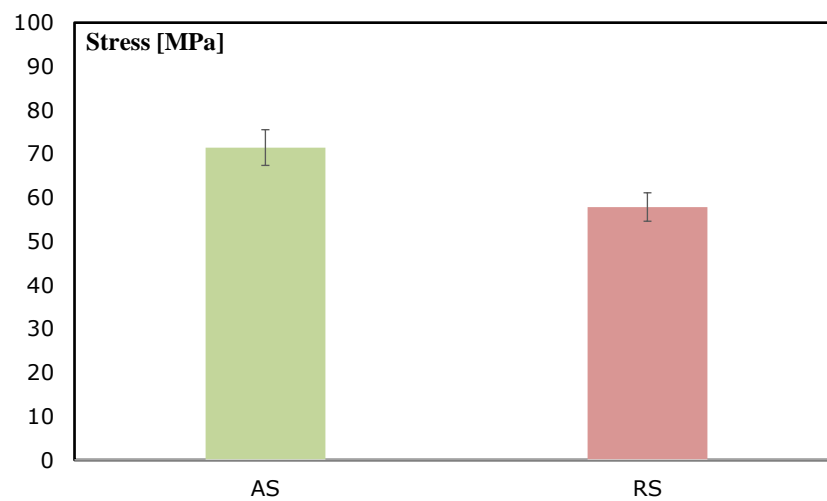


Figure 7. Comparison between the maximum stresses for AS and RS joints.

This different behavior can be explained by analyzing the effect of heat transfer during the process and the presence of residual stresses. For the RS samples, the generated heat is not enough to guarantee an adequate plastic deformation of the steel, making the welding process difficult [18].

Temperatures and deformations also influence the level of residual stresses that are connected to the different positions of the tool. Variations in the residual stress profile could be related to the differences in the mechanical properties and its susceptibility to retreating or advancing sides, which promote different behaviors in the materials when they are subjected to the same welding conditions. Although the difference in magnitude of the residual stresses in the advancing and retreating sides is not relevant, several authors present the maximum residual stresses in the advancing side or observe the maximum longitudinal stresses in the advancing side for different transverse speeds [19,20].

In addition, one of the main factors affecting the tensile strength of the friction stir welded lap joint is the sheet interface shape (i.e., hooking): in lap joints, due to the mutual position of the two sheets to be welded, the welding surface should be horizontal. Really, the welding surface after the joining process is not perfectly horizontal and flat, because the material flow causes a wavy bonding surface [21,22]. This effect is significant for the strength of dissimilar friction stir welded lap joints because it can represent an interpenetrating feature creating mechanical interlocking conditions [23]. This interlocking can enhance the tensile strength [24] if it involves homogeneously the whole interface. Otherwise, it can negatively affect the mechanical properties [25] due to the presence of local hooks promoting start and crack propagation.

Particularly, Figure 5b shows on the typical fracture area of a RS sample several local hooks that are not evident in the typical fracture area of an AS sample (Figure 5a). In his last case, the interlocking involves the mixing paths induced by the tool on the whole interface.

3.2. Hardness Test

The hardness profiles as a function of the distance from the joint interface for both AS and RS were carried out. Figure 8 shows the microhardness evolution along the cross section of the FSW joints at varying the distance from the joint surface, both along steel and aluminum sheets. The profiles exhibit non-symmetrical trends due to the different mechanical and physical properties of dissimilar base materials. The hardness profiles also indicate the existence of an interfacial area between the aluminum alloy and the steel sides in the stirred zone (indicated as SZ in Figure 8) for both AS and RS samples. Indeed, four zones can be identified after the FSW process: the base metals, the stir zone (SZ), the thermo-mechanical affected zone (TMAZ), and the heat-affected zone (HAZ). According to the present results, the hardness values on the aluminum side were almost constant in

all directions because the aluminum base metal is a non-heat-treatable, work-hardened aluminum alloy [26]. This behavior is in accordance also with [27,28]. Moreover, Vijayan et al. [29] evidence that the formation of working hardening zone depends on the material flow behavior under the action of the rotating tool in terms of geometry and process parameters. Consequently, the characteristics of the tool, used in the present work, are not enough to induce the formation of this specific area.

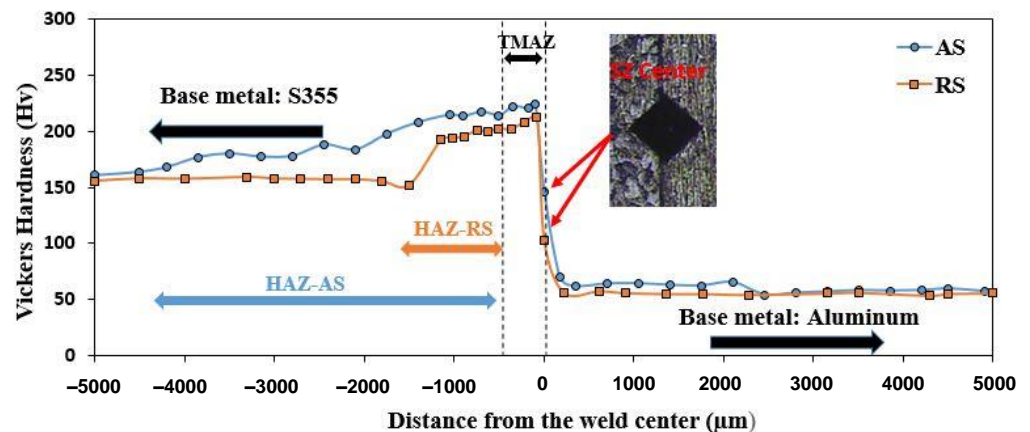


Figure 8. Mean Hardness profiles of AS and RS perpendicular to the AW 5083/S355 interface.

Thus, there is no significant FSW effect on the hardness of the aluminum, inducing the absence of HAZ in this metal. The average hardness of the aluminum zone (base metal) is around 55 HV_{0.5}, while it is 158 HV_{0.5} in the base steel. The highest values of hardness were observed on steel TMAZ. The maximum value of hardness reached in this zone is about 212 HV_{0.5} for the RS and 220 HV_{0.5} for the AS. Then the hardness gradually decreases in the direction of the HAZ, but it is still higher than the base steel. It is clear that the HAZ of the AS is larger than the RS, and the hardness reached higher values for this type of sample, confirming the previous mechanical results.

In addition, the narrow HAZ formed in the steel regions, is due to rapid cooling from the estimated peak temperature down to the atmosphere, resulting in higher hardness than the base metal. To understand this difference in the hardness behavior of the metallographic microstructures of the different regions, see [8].

The results showed that grain structure has the possibility to deform during the FSW process. The grain structure in TMAZ, HAZ and especially in the SZ region is largely refined, which explains the difference in hardness values. The SZ and affected zones (TMAZ, HAZ) have a smaller grain size than the steel base metal due to the recrystallization of these grains when heated by the tool stirring action. In addition, the affected zones are modified by the recrystallization of steel grains. In fact, the main controlling mechanisms for such grain structural modification are based on the operative dynamic restoration phenomena during the FSW process. The involved mechanisms mostly include dynamic recovery (DRV), geometric dynamic recrystallization (GDRX), and continuous dynamic recrystallization (CDRX) [30,31]. In fact, the grains can nucleate during the plastic deformation of the FSW process, and then the cooling from a peak temperature after the welding process will induce the grain growth, and the rate of grain boundaries' migration induces the formation of a finer grain structure in the steel side of dissimilar weld.

3.3. Microstructural Characterization

To deepen the correlation between the mechanical properties and the morphology of the aluminum/steel welds, a detailed study of the microstructure was carried out. Cross-section of the dissimilar metal joint was observed by scanning electron microscopy (SEM).

The formation of a thin intermetallic compound (IMC) layer (light gray area shown by the blue arrow in Figure 9) at the aluminum and steel interface can be clearly observed. The IMC was formed due to the frictional heating on the surface under the action of the

rotating shoulder [32]. Some fragments scattered in the Al matrix were also formed. The EDS analyses indicated that these fragments are steel-based ones. This phenomenon is due to the rotation effect of the pin, which pulled small pieces of steel from the surface and scattered them on the aluminum surface. Furthermore, due to the difficulty of inserting the soft metal (aluminum) into the hard metal (steel), there is no obvious presence of aluminum fragments or particles in the steel side [33].

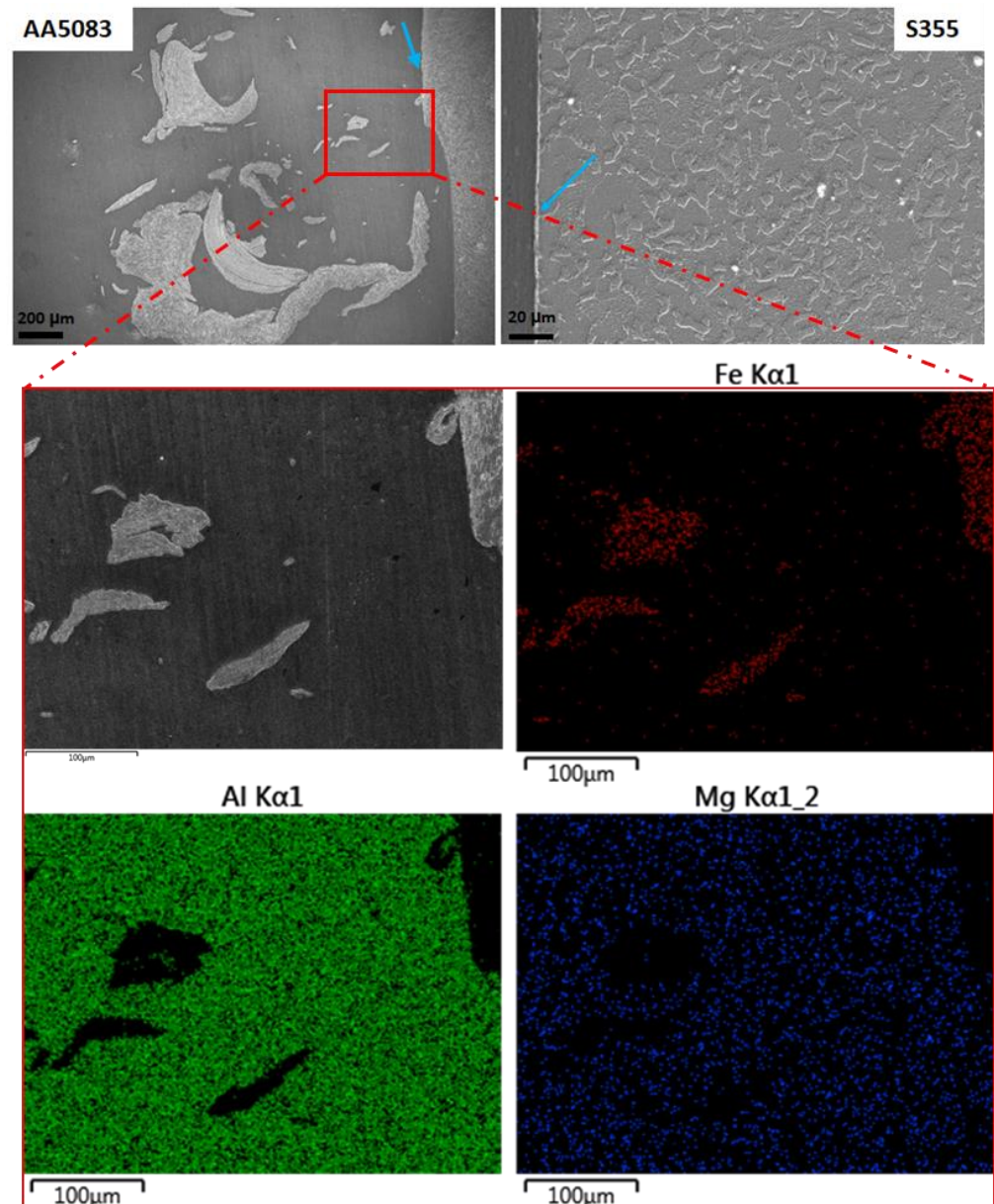


Figure 9. SEM images of the Al/steel joint cross section and EDS maps near the weld interface.

The quantity and shape of these steel fragments are determined by the weld side. In fact, Figure 10 shows that the fragments of steel on the advancing side are larger than the retreating one. Furthermore, the amount of these fragments on the retreating side is lower than on the advancing side; this could be because the steel is highly deformed on the side relative to the advancing joining line and the tool can pull off larger parts of steel. This may also justify the hardness behavior where the HAZ in the AS is larger and harder than the RS.

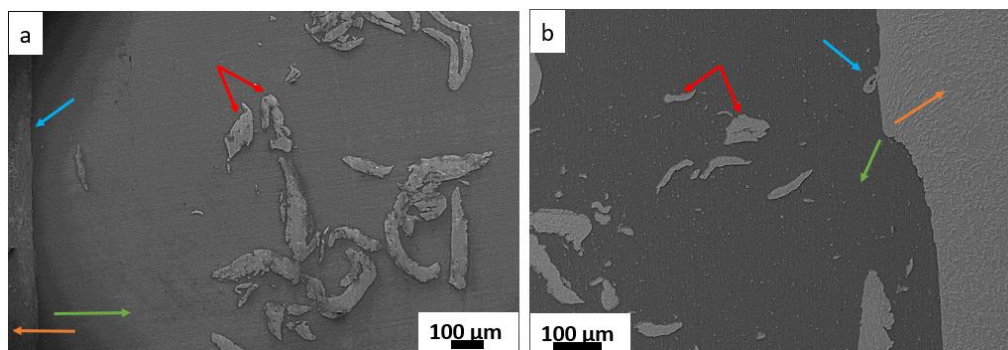


Figure 10. SEM images of the advancing (a) and retreating (b) sides (AA 5083 showed by the green arrows, S355 showed by the orange arrows, the intermetallic layer showed by the blue arrows and the steel fragments scattering in the Al matrix showed by the red arrows).

4. Statistical Analysis

With the Minitab® software (v17.1.0, Minitab LCC, State College, PA, USA), a variance analysis was performed aiming to evaluate if the difference in mechanical properties between the joint realized in advancing side and that realized in retreating side is significant.

In Figure 11, the distribution of data and residual were checked showing a normal distribution and a random distribution of residuals versus fits.

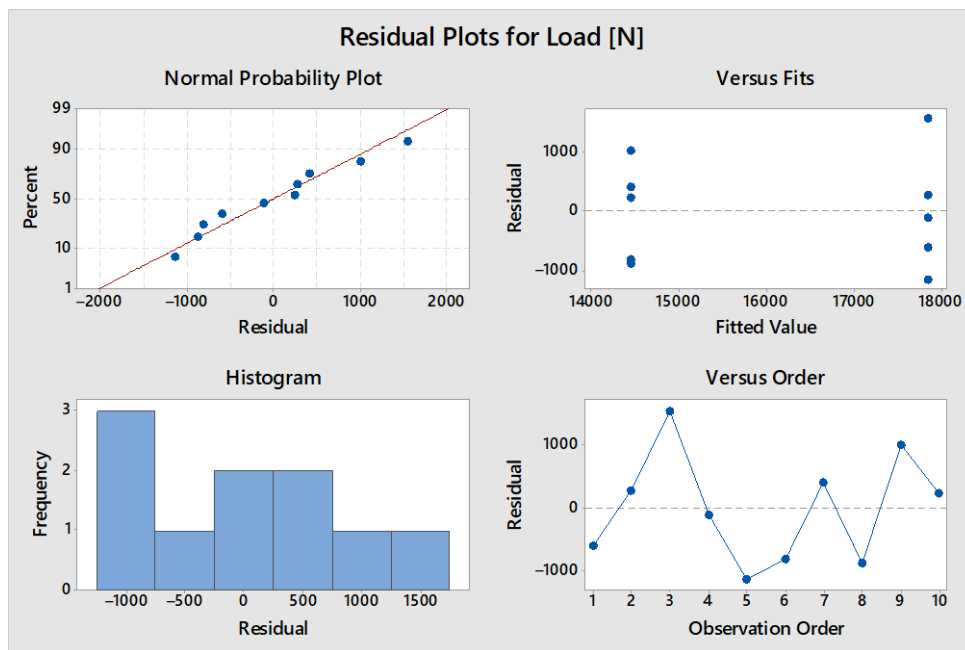


Figure 11. ANOVA—Distribution of data and residual.

Whereas Table 3 summarizes the main results of the variance analysis by considering that one single parameter (i.e., maximum load) was investigated by varying it on two levels (i.e., the advancing and retreating sides).

Table 3. ANOVA: Analysis of Variance for Maximum Load [N].

Source	DF	SS	MS	F	p
Side	1	28,848,087	28,848,087	3381	0.000
Error	8	6,826,656	853,332		
Total	9	35,674,743			
S = 923.760		R-Sq = 80.86%		R-Sq(adj) = 78.47%	

DF are the degrees of freedom, used to calculate the mean square (MS). In general, they measure how much ‘independent’ information is available to calculate each sum of squares (SS). This last, also called sum of the squared deviations, measures the total variability in the data, which is made up of the following sources: (i) the SS for each of the two factors, which measures how much the level means differ within each factor; (ii) the SS for the interaction, that measures how much the effects of one factor depend on the level of the other factor and (iii) the SS for error, that measures the variability that remains after the factors and interaction are taken into account. MS is simply SS divided by the degrees of freedom. The MSs for error is an estimate of the variance in the data left over after differences in the means were accounted. F is used to determine the p -value (p) that defines if the effect for a term is significant: i.e., if p is less than or equal to a selected level (i.e., 0.05, corresponding to a 95% level of confidence), the effect for the term is significant.

From the results, it is evident that the value of probability is less than the value of 0.05, which indirectly proves that the developed model is satisfactory [34]. Consequently, it is possible to affirm that the variable (i.e., side) has effect on the maximum load.

The S value is very low with respect to the values of the response variable, showing a good description of the model of the response. The R² value is the percentage of variation in the response explained by the model.

5. Conclusions

A friction stir welded single lap joint between steel and aluminum was investigated in this work. It is possible to deduce from the results, in particular:

- By varying the side (i.e., advancing or retreating), the mechanical properties change: the advancing side joints are characterized by a higher joint strength than the retreating side ones. This process parameter affects temperatures, deformations, residual stresses, interlocking at interface (i.e., hooking effect) and, consequently, the mechanical properties.
- Microstructure analyses evidence that of a thin intermetallic compound (IMC) layer at the aluminum and steel interface can be clearly observed due to the rotation effect of the pin, which pulled small pieces of steel from the surface and scattered them on the aluminum surface. By changing the weld side, the quantity and shape of these steel fragments change by affecting the mechanical behavior.
- Finally, the statistical analysis demonstrates that difference in the mechanical behavior between AS joints and RS ones is significant.

This fact has a significant implication in the production of joints that must be employed in shipbuilding in substitution of traditional welding or explosion welding, both if the joint is provided by an outsourced supplier and if the joint is directly produced in the shipyard.

Further studies on this joint focus on the ageing of seawater to determine how corrosion phenomena affect joint strength. Other studies, such as fatigue resistance, are less significant. In fact, this joint between dissimilar metals is not used in areas of the ship where vibrations can cause fatigue failures (such as the engine room), but rather in areas where the effect of vibrations is less noticeable, but the corrosion caused by the different metals is more severe.

Author Contributions: Conceptualization, G.D.B., C.B. and E.P.; methodology, G.D.B. and A.K.; formal analysis, G.D.B. and A.K.; investigation, G.D.B., C.B. and A.K.; resources, G.D.B.; data curation, A.K.; writing—original draft preparation, A.K. and G.D.B.; writing—review and editing, G.D.B. and A.K.; visualization, G.D.B.; supervision, C.B. and E.P.; project administration, G.D.B. and E.P.; funding acquisition, E.P. All authors have read and agreed to the published version of the manuscript.

Funding: This research was funded by Sicilian Region on the European Regional Development Fund 2014-2020, as part of the project “Soluzioni Innovative per Mezzi navali ad Alto Risparmio Energetico (SI-MARE)”, grant number 08ME7219090182.

Data Availability Statement: Not applicable.

Conflicts of Interest: The authors declare no conflict of interest. The funders had no role in the design of the study; in the collection, analyses, or interpretation of data; in the writing of the manuscript; or in the decision to publish the results.

References

1. Shankar, S.; Mehta, K.P.; Chattopadhyaya, S.; Vilaça, P. Dissimilar friction stir welding of Al to non-Al metallic materials: An overview. *Mater. Chem. Phys.* **2022**, *288*, 126371. [[CrossRef](#)]
2. Chauhan, G.; Sahu, M.; Prasad, P.; Paul, A.; Ganguly, S. Effect of process parameters on friction stir welded joints of AA 7039. *Mater. Today Proc.* **2022**, *66*, 566–572. [[CrossRef](#)]
3. Sahu, M.; Ganguly, S. Distribution of intermetallic compounds in dissimilar joint interface of AA 5083 and HSLA steel welded by FSW technique. *Intermetallics* **2022**, *151*, 107734. [[CrossRef](#)]
4. Giallanza, A.; Marannano, G.; Morace, F.; Ruggiero, V. Numerical and experimental analysis of a high innovative hydrofoil. *Int. J. Interact. Des. Manuf.* **2020**, *14*, 43–57. [[CrossRef](#)]
5. Fragapane, S.; Giallanza, A.; Cannizzaro, L.; Pasta, A.; Marannano, G. Experimental and numerical analysis of aluminum-aluminum bolted joints subject to an indentation process. *Int. J. Fatigue* **2015**, *80*, 332–340. [[CrossRef](#)]
6. Mao, Y.; Qin, D.; Xiao, X.; Wang, X.; Fu, L. Achievement of high-strength Al/Cu dissimilar joint during submerged friction stir welding and its regulation mechanism of intermetallic compounds layer. *Mater. Sci. Eng. A* **2022**, *865*, 144164. [[CrossRef](#)]
7. Gullino, A.; Matteis, P.; D’Aiuto, F. Review of Aluminum-To-Steel Welding Technologies for Car-Body Applications. *Metals* **2019**, *9*, 315. [[CrossRef](#)]
8. Khaskhoussi, A.; Di Bella, G.; Borsellino, C.; Calabrese, L.; Proverbio, E. Microstructural and electrochemical characterization of dissimilar joints of aluminum alloy AW5083 and carbon steel S355 obtained by friction welding. *Metall. Ital.* **2022**, *9*, 15–21.
9. Colwell, K.C. Two metals enter, one leaves: The miracle of friction stir welding. *Car Drive.* **2013**, *15*.
10. Kusuda, Y. Honda develops robotized FSW technology to weld steel and aluminum and applied it to a mass-production vehicle. *Ind. Robot.* **2013**, *40*, 208–212. [[CrossRef](#)]
11. Ohhama, S.; Hata, T.; Yahaba, T.; Kobayashi, T.; Miyahara, T.; Sayama, M. *Application of an FSW Continuous Welding Technology for Steel and Aluminum to an Automotive Subframe*; SAE International: Warrendale, PA, USA, 2013. [[CrossRef](#)]
12. Mishra, R.S.; Ma, Z.Y. Friction stir welding and processing. *Mater. Sci. Eng. R Rep.* **2005**, *50*, 1–78. [[CrossRef](#)]
13. Thomas, W.; Nicholas, D.; Staines, D.; Tubby, P.J.; Gittos, M.F. FSW Process Variants and Mechanical Properties. *Weld. World* **2004**, *49*, 4–11. [[CrossRef](#)]
14. Zhang, H.; Wang, M.; Zhang, X.; Zhu, Z.; Yu, T.; Yang, G. Effect of Welding Speed on Defect Features and Mechanical Performance of Friction Stir Lap Welded 7B04 Aluminum Alloy. *Metals* **2016**, *6*, 87. [[CrossRef](#)]
15. Di Bella, G.; Alderucci, T.; Favaloro, F.; Borsellino, C. Effect of tool tilt angle on mechanical resistance of AA6082/AA5083 friction stir welded joints for marine applications. In Proceedings of the 16th CIRP Conference on Intelligent Computation in Manufacturing Engineering (CIRP ICME 2022), Naples, Italy, 13–15 July 2022.
16. Di Bella, G.; Alderucci, T.; Salmeri, F.; Cucinotta, F. Integrating the sustainability aspects into the risk analysis for the manufacturing of dissimilar Aluminium/Steel Friction Stir Welded single lap joints used in marine applications through a Life Cycle Assessment. *Sustain. Futures* **2022**, *4*, 100101. [[CrossRef](#)]
17. Yao, H.; Chen, K.; Kondoh, K.; Dong, X.; Wang, M.; Hua, X.; Shan, A. Microstructure and mechanical properties of friction stir lap welds between FeCoCrNiMn high entropy alloy and 6061 Al alloy. *Mater. Des.* **2022**, *224*, 111411. [[CrossRef](#)]
18. Sivasankara, R.R.; Jagadish; Rao, C.J.; Aadapa, S.K.; Yanda, S. Predication of temperature distribution and strain during FSW of dissimilar Aluminum alloys using Deform 3D. *Mater. Today Proc.* **2022**, *59*, 1760–1767.
19. Zapata, J.; Toro, M.; Lopez, D. Residual stresses in friction stir dissimilar welding of aluminum alloys. *J. Mater. Process. Technol.* **2016**, *229*, 121–127. [[CrossRef](#)]
20. Brewer, L.N.; Bennett, M.S.; Baker, B.W.; Payzant, E.A.; Sochalski-Kolbus, L.M. Characterization of residual stress as a function of friction stir welding parameters in oxide dispersion strengthened (ODS) steel MA956. *Mater. Sci. Eng. A* **2015**, *647*, 313–321. [[CrossRef](#)]
21. Buffa, G.; Campanile, G.; Fratini, L.; Prisco, A. Friction stir welding of lap joints: Influence of process parameters on the metallurgical and mechanical properties. *Mater. Sci. Eng. A* **2009**, *519*, 19–26. [[CrossRef](#)]
22. Astarita, A.; Tucci, F.; Silvestri, A.T.; Perrella, M.; Boccarusso, L.; Carlone, P. Dissimilar friction stir lap welding of AA2198 and AA7075 sheets: Forces, microstructure and mechanical properties. *Int. J. Adv. Manuf. Technol.* **2021**, *117*, 1045–1059. [[CrossRef](#)]
23. Dubourg, L.; Merati, A.; Jahazi, M. Process optimisation and mechanical properties of friction stir lap welds of 7075-T6 stringers on 2024-T3 skin. *Mater. Des.* **2010**, *31*, 3324–3330. [[CrossRef](#)]
24. Naik, B.S.; Chen, D.L.; Cao, X.; Wanjara, P. Microstructure and Fatigue Properties of a Friction Stir Lap Welded Magnesium Alloy. *Metall. Mater. Trans. A* **2013**, *44*, 3732–3746. [[CrossRef](#)]
25. Chowdhury, S.H.; Chen, D.L.; Bhole, S.D.; Cao, X.; Wanjara, P. Lap shear strength and fatigue behavior of friction stir spot welded dissimilar magnesium-to-aluminum joints with adhesive. *Mater. Sci. Eng. A* **2013**, *562*, 53–60. [[CrossRef](#)]
26. Elrefaey, A.; Gouda, M.; Takahashi, M.; Ikeuchi, K. Characterization of aluminum/steel lap joint by friction stir welding. *J. Mater. Eng. Perform.* **2005**, *14*, 10–17. [[CrossRef](#)]

27. Koilraj, M.; Sundareswaran, V.; Vijayan, S.; Rao, S.R.K. Friction stir welding of dissimilar aluminum alloys AA2219 to AA5083—Optimization of process parameters using Taguchi technique. *Mater. Des.* **2012**, *42*, 1–7. [[CrossRef](#)]
28. Gungor, B.; Kaluc, E.; Taban, E.; Sik, A. Mechanical, fatigue and microstructural properties of friction stir welded 5083-H111 and 6082-T651 aluminum alloys. *Mater. Des.* **2014**, *56*, 84–90. [[CrossRef](#)]
29. Vijayan, S.; Raju, R.; Rao, S.R.K. Multiobjective Optimization of Friction Stir Welding Process Parameters on Aluminum Alloy AA 5083 Using Taguchi-Based Grey Relation Analysis. *Mater. Manuf. Process.* **2010**, *25*, 1206–1212. [[CrossRef](#)]
30. McNelley, T.R.; Swaminathan, S.; Su, J.Q. Recrystallization mechanisms during friction stir welding/processing of aluminum alloys. *Scr. Mater.* **2008**, *58*, 349–354. [[CrossRef](#)]
31. Elnabi, M.M.A.; Osman, T.A.; Mokadem, A.E.; Elshalakany, A.B. Evaluation of the formation of intermetallic compounds at the intermixing lines and in the nugget of dissimilar steel/aluminum friction stir welds. *J. Mater. Res. Technol.* **2020**, *9*, 10209–10222. [[CrossRef](#)]
32. Martinsen, K.; Hu, S.J.; Carlson, B.E. Joining of dissimilar materials. *CIRP Ann. Manuf. Technol.* **2015**, *64*, 679–699. [[CrossRef](#)]
33. Tanaka, T.; Nezu, M.; Uchida, S.; Hirata, T. Mechanism of intermetallic compound formation during the dissimilar friction stir welding of aluminum and steel. *J. Mater. Sci.* **2020**, *55*, 3064–3072. [[CrossRef](#)]
34. Satheesh, C.; Sevel, P.; Kumar, R.S. Experimental Identification of Optimized Process Parameters for FSW of AZ91C Mg Alloy Using Quadratic Regression Models. *Stroj. Vestn. J. Mech. Eng.* **2020**, *66*, 736–751.

Disclaimer/Publisher’s Note: The statements, opinions and data contained in all publications are solely those of the individual author(s) and contributor(s) and not of MDPI and/or the editor(s). MDPI and/or the editor(s) disclaim responsibility for any injury to people or property resulting from any ideas, methods, instructions or products referred to in the content.